AERODYNAMIC ANALYSIS OF THE FUSELAGE OF A FIXED WING AIRCRAFT TYPE UAV USING THE FINITE ELEMENT METHOD

Second lieutenant engineer Cătălin CUCU

Faculty of Industrial Engineering and Robotics, Master: Conception Intégrée de Systèmes Technologiques, 1st Year of study, e-mail: ionut.cucu@mta.ro

Scientific coordinator: Prof. PhD. Eng. Cristina PUPĂZĂ

ABSTRACT: Nowadays the unmanned aerial vehicles are employed on a large scale, from military to industry implementations, from battlefields to smaller units that people may be play outdoor. The military industry drones recorded an exponentially growth worldwide since '90s. They are used in missions that are dangerous for humans and can stay in the air for a large period of time. The UAVs have a complex cross-section shape of the fuselage. This paper explores the aerodynamic consequences of its shape, at the operational flight ceiling, in a comparative approach, using Computational Fluid Dynamics (CFD).

KEYWORDS: aerodynamic, CFD, UAV, fuselage, Spalart-Allmaras.

1. Introduction and state of art

The unmanned aerial vehicles (UAV) have touched a level of development without precedent and spread throughout the world massively. In the next twenty years they will take control on the battlefield. From a strategic point of view, from 1997 the United States of America published a long-term development plan, which was later modified so that one can talk today about a hierarchy of UAVs according to the destination, battlefield response capabilities and the conventional level of operation [1].

One of the first applications of an UAV was in the first Gulf War. In Iraq, eight years later, the allied forces employed three UAVs for surveillance and aerial research of the battlefield [1], [2]. Afghanistan was another battlefield where three UAVs RQ-1 Predator were used, but their mission was only combat and surveillance. The U.S. Army analysis showed that in 2006, 46% of the UAVs capacity requirement was not accomplished, especially with the correct location of the ground target acquisition and the precision of the attack.

The purpose of this study is to examine the status of the technological development in the domain and to make a comparison of the different types of designs. Drones are conceived and manufactured according to their mission and can perform some of the following tasks [1], [3], [4], [5]:

- Surveillance - representing the process of monitoring humans, objects, or processes behavior, to be compared to the expected or required norms (for example detecting chemical, biological or nuclear activities or phenomena).
- Reconnaissance - represents the scan or inspection of an area to obtain information.
- Insertion - is the activity for load delivery in specific areas for example weapons airdropping (not necessarily lethal), electronic war actions and target destruction actions. The electronic war actions can have two characteristics: the attack against the enemy, for the electronic jamming or by high energy weapon bombing of the convoys, and the protection of their own and allied communications, equipment, or objectives.
- Target - represented by an UAV that can be used to replicate a fighter aircraft or a missile in the following purposes:
  a. Training for operators, in this case the UAV being considered as a practical target
  b. Reproduce an aerial vehicle to take advantage of the surveillance devices of the enemy, in this case being used as a trap.

UAVs could be classified depending on the action range/altitude and as agreed within some industry events in [1]:

- handheld UAV – 600 m altitude and action range of about 5 km.
- close range UAV – 1500 m altitude and action range of about 10 km.
- NATO – 3000 m altitude and the action range of about 50 km.
- tactical (TUAV) – 5500 m altitude and action range of about 160 km.
- MALE (Medium Altitude, Long Endurance) – up to 9000 m altitude and action range of 200 km.
- HALE (High Altitude, Long Endurance) – above 9000 m altitude and unlimited action range.
- HYPERSONIC – high speed, supersonic (1 – 5 Mach) or hypersonic (above 5 Mach), flight altitude of more than 15200 m or sub-orbital altitude, having the action range of more than 200 km.

Under these circumstances, one of the most important advantages of the UAVs is their ability to remote control, which has made them popular in the aviation industry and especially in the military industry. The design of UAVs requires special attention due to the fact that the evolution in flight and its control is done remotely. Thus, great efforts are done on the structural design of these vehicles and in particular in their aerodynamic design. Simulating the air flow around the UAV is of great importance for studying the aerodynamic forces and stability of the aircraft during flight in order to determine optimal models to suit the missions they have to accomplish. The use of the Finite Element Simulation (FEM) software such as ANSYS Fluent can significantly reduce the costs of the design, construction and testing of these complex structures.

2. Presentation of models

Following a preliminary study conducted on a sample of twenty aircrafts, three reference aircrafts were chosen, the CAD models were generated in order to be analyzed in ANSYS Fluent software from the aerodynamic point of view.

Model one

Fig. 1. Model one

Fig. 2. Elbit Hermes 900 [6]

The Hermes 900 is a high-endurance UAV flying at medium altitude, designed by the Israeli company Elbit Systems to perform different types of tactical missions. They have been in service since 2012. The positioning of the wing is in the central part of the fuselage, the empennage is in the shape of a "V", and the propeller is driven by a Rotax 914 four-cylinder piston engine that develops a power of 86 kW (115 hp). The aircraft can be equipped with a radar system for tracking moving targets, intelligent electrical and communication system, electronic warfare system and hyperspectral sensors. [7].

Model two

Fig. 3 Model two

Fig. 4 Orion UAV [8]

The Orion UAV is a high-endurance unmanned aircraft operating at medium altitude. The position of the wing is intermediate, with an empennage in "V" and the propeller of the propulsion system positioned behind the empennage. Developed by the Russian company Kronshtadt Group as a reconnaissance system with equipment for mapping the terrain, identification, and transmission of the coordinates of the target, its design is similar to the MQ-1 Predator and MQ-9 Reaper aircraft.

The aircraft is equipped with a Rotax 914 piston engine with a power of 86 kW (115 hp), equipped with a turbocharger, a fixed angle of attack propeller of type AV-115 with a diameter of 1.9m. A complete Orion system consists of 6 UAVs, the control station, the communication network, and the launch system. [9]

Model three

Fig. 5. Model three

Fig. 6. MQ-4C Triton [10]

The Northrop Grumman MQ-4C Triton is a high-endurance aircraft operating at high altitudes in development for the U.S. Navy for surveillance purposes. The position of the wing is median, with empennage in "V" shape, and the propulsion system consists of a Rolls-Royce AE 3007 turbo-engine with a maximum traction of 40 kN. It can carry distinct types of sensors such as: thermal imaging camera (infrared) and aerial surveillance of ground targets. It employs an autonomous take-off and landing system, different types of radars and an automatic control system to return to the control center in case the radio connection is lost. [11]

The three CAD models presented above are similar, having the same wing, V empennage, surveillance devices, propellers, intake device and exhaust device, the difference being the shape and cross-sectional area of the fuselage so that the analysis is conducted under the same conditions and the results obtained can be compared strictly from this point of view.

Geometric features of the models

- The length of the fuselage is about 8.5 m for the three models.
- The wingspan is 17.3 m.
- The half-wingspan of the empennage V is 1.2 m.
- The diameter of the propeller is 3 m.
- The average diameter of the cross-sections of the fuselage is 0.84 m, 0.61 m, and 0.92 m.

3. Analytical approach to the phenomenon of fluid flow around an aerodynamic profile

Aerodynamic drag force is caused by the dynamic interaction between a body surface and the fluid which flows over it. Two major terms which govern the aerodynamic drag and lift coefficients are the normal stress and wall shear stress. Pressure distribution dominates the normal stresses acting on the body surface, while surface roughness contributes to the wall shear stress. The equations needed for calculating the lift and drag coefficients are remarkably similar. The lift force that an airfoil generates depends on the density of the air, the velocity of the airflow, the dynamic viscosity and the compressibility of the air, the surface area of the airfoil, the shape of the airfoil, and the airfoil's angle of attack. However, dependence on the airfoil's shape, the angle of attack, air viscosity and compressibility are very complex. Thus, they are characterized by a single variable in the lift equation, called the lift coefficient, so the lift equation is given by the equation (1). [12], [13]

Similar with to the lift coefficient, the drag coefficient of an airfoil depends on the air density, the velocity of the airflow, the viscosity and compressibility of the air, the surface area of the airfoil, the

shape of the airfoil, and the angle of attack [12], [13]. The drag coefficient is generally found through testing in a wind tunnel, where the drag can be measured, and the drag coefficient is calculated by rearranging the equation (2). [12], [13]

$$L = \frac{1}{2}\rho U^2 S c_L \quad (1)$$

$$D = \frac{1}{2}\rho U^2 S c_D \quad (2)$$

where
L is the lifting force [N]
D is the drag force [N]
ρ is the density of air [kg/m^3]
U is the relative velocity of the airflow [m/s]
S is the reference area of the airfoil [m^2]
c_L is the lift coefficient
c_D is the drag coefficient.

Lift coefficient

The lift coefficient for a wing at a specified angle of attack and for specific flow conditions can be determined using the following equation [12], [13]:

$$c_L = \frac{L}{\frac{1}{2}\rho U^2 S} \quad (3)$$

Drag coefficient

In fluid dynamics the drag coefficient commonly denoted as c_D is a dimensionless quantity that is used to quantify the drag or resistance of an object in a fluid environment such as air or water. It is used in the drag equation where a lower drag coefficient indicates the object will have less aerodynamic or drag, it is always associated with a particular surface area. This parameter takes in consideration the effects of the body shape, air properties such as viscosity and compressibility. Drag coefficient can be determined using the following equation [12], [13]:

$$c_D = \frac{D}{\frac{1}{2}\rho U^2 S} \quad (4)$$

4. Description of the cross-section shape of the models

To achieve the cross-section shape of the models, a super-ellipse function was implemented in the MATLAB software:

$$Y = C * Z^{N_1} * (1 - Z)^{N_2}, \quad (5)$$

where

$Z = [0,1]$,

N_1 *is a coefficient for the curvature of the lower part*,

N_2 *is a coefficient for the curvature of the upper part*,

C *is a scaling coefficient*.

The CAD model was created in CATIA V5 software by importing four hundred points, which were calculated in MATLAB software, in the characteristic sections of the model aircrafts (Fig. 7, Fig. 8, Fig. 9).

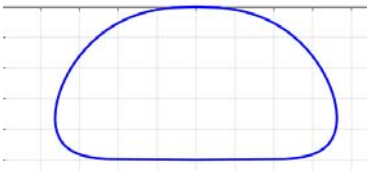

Fig. 7. Model one: Shape of the cross-section in MATLAB

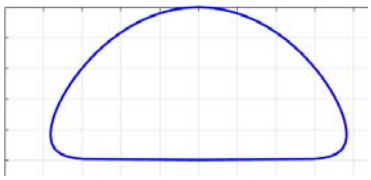

Fig. 8. Model two: Shape of the cross-section in MATLAB

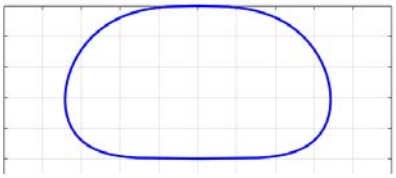

Fig. 9. Model three: Shape of the cross-section in MATLAB

5. Geometry and mesh of the fluid flow domain

The fluid flow domain was designed around a half of the models and has a structured poly-hexacore mesh which was generated in ANSYS Fluent 2021 R1. The eight inflation layers are uniform and for each major part of the aircrafts the first layer and the growth ratio were computed for accurate results of turbulence close to the walls. All three domains have approximately 3.5 million elements (Fig. 10 to Fig. 12).

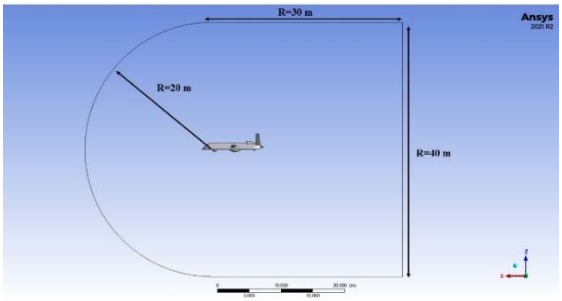

Fig. 10. Domain dimensions

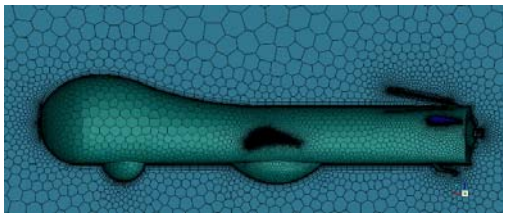

Fig. 11. Close view of domain mesh

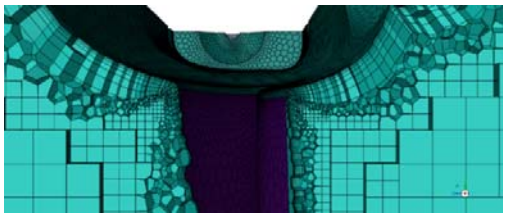

Fig. 12. Section view with inflation layers

6. Boundary conditions

For the CFD steady state analysis the Spalart-Allmaras turbulence model was employed, with a one equation Reynolds-Averaged Navier-Stokes (RANS) turbulence model. This model was chosen for the following reasons.

The k-ε model was proposed in the early 1970s, so this is the oldest of the turbulence models. It is used fairly widely in a variety of engineering disciplines but what was found when the k-ε was originally proposed and continues to be noticed today is that the k-ε model is not accurate at predicting boundary layer flows with adverse pressure gradients. So that it is particularly challenging for airfoils and wings at high angle of attack and for turbomachinery applications. The k-ε model tends to get even worse when shocks are present because it increases the strength of the adverse pressure gradient. Based on this observation it is desirable to have a better turbulence model, particularly for these applications and that is where the new model tends to come in.

The Spalart-Allmaras turbulence model was proposed in 1994 and it is fairly significant that this model is about the same as the k-ω model, which was proposed in 1988 and was essentially the same as the k-ω SST model. These models were simultaneously proposed, and they all aim to identify and help to improve the prediction of the same class of flows, which were the boundary layer flows subject to adverse pressure gradients.

Often the k-ω SST model is preferred to the Spalart-Allmaras for the majority of aerodynamic applications and this is mainly because both models were introduced at the same time, around 1994. However, since at that time a lot of comparative testing by a variety of groups was performed, generally the k-ω SST model has been found to give a better behavior. Therefore that is why for the majority of simulation attempts, the k-ω SST model tends to be employed and preferred. It is now recommended in most cases. But this model is much more computational expensive than the Spalart-Allmaras turbulence model which is a very straightforward and simple model to be implemented in the CFD aerodynamic applications. We expect to obtain satisfactory results using this model [14], [15], [16].

The test case analyzed in this research involved the atmospheric conditions of the flight ceiling of 10,000 m, the angle of attack of the air flow of 5° and the air flow velocity of 60 m/s.

The dynamic viscosity and density of the working fluid were considered constants, the Mach number is 0.2 and the Reynolds number is approximately the same for the three models, 1,344,000.

Table 1. Air proprieties at 10,000 m

Air proprieties at 10,000 m	
Density	0.412707 kg/m^3
Temperature	223,15 K
Pressure	26436,3 Pa
Viscosity	1,469 Pa*s
Sound speed	299,463 m/s

7. Comparison of the results achieved for the three models

The static pressure distribution

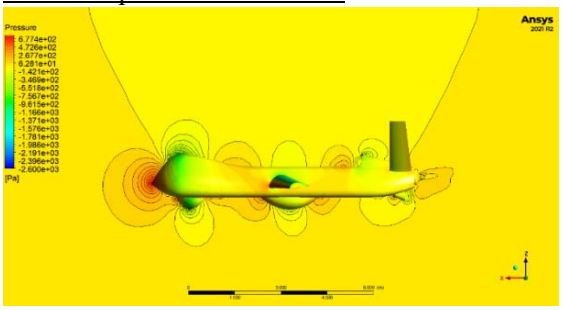

Fig. 13. Detailed close view of static pressure Model one

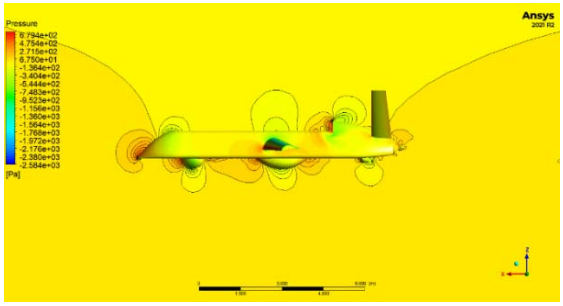

Fig. 14 Detailed close view of static pressure Model two

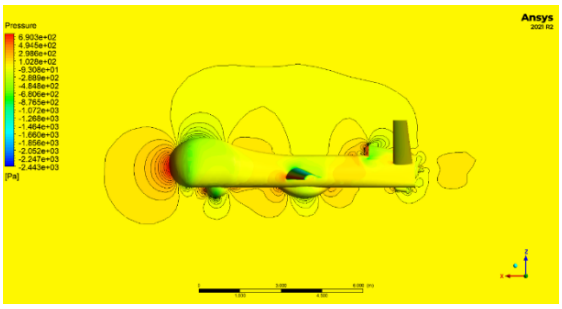

Fig. 15. Detailed close view of static pressure Model three

Velocity distribution

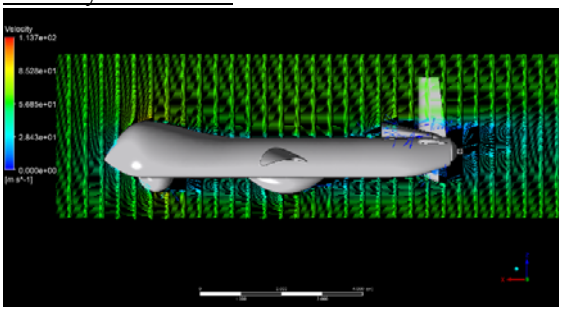

Fig. 16. Vertical velocity distribution Model one

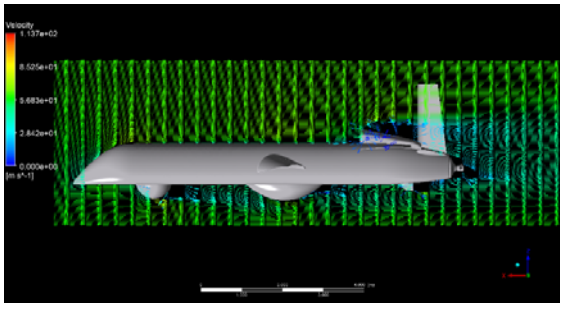

Fig. 17. Vertical velocity distribution Model two

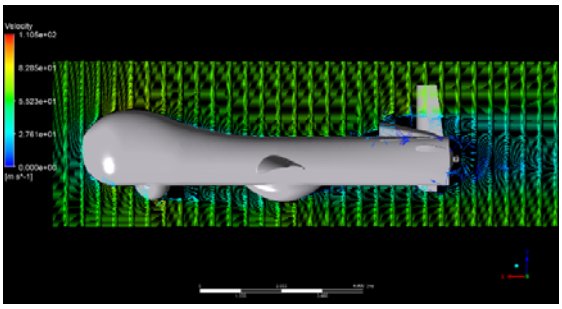

Fig. 18 Vertical velocity distribution Model three

Eddy viscosity distribution

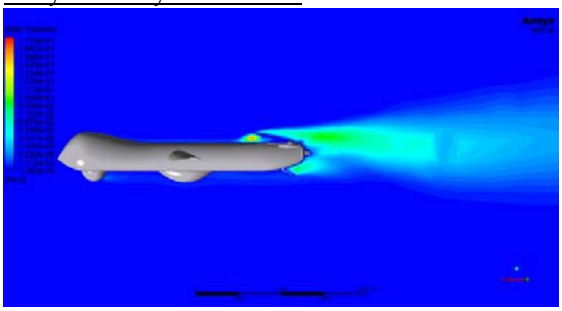

Fig. 19. Close view of eddy viscosity Model one

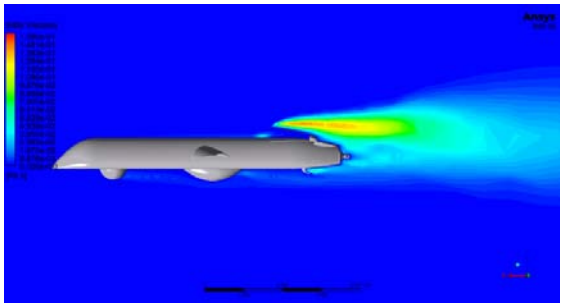

Fig. 20. Close view of eddy viscosity Model two

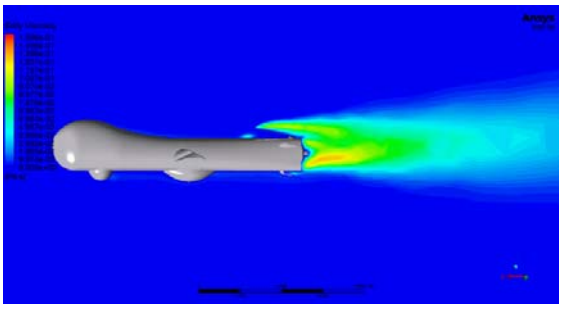

Fig. 21. Close view of eddy viscosity Model three

Comparison according to the distribution of static pressure:

- The first model has the lowest value of the static pressure which can be transposed in the lowest drag force, because the leading edge of the fuselage is sharp.
- The third model has the higher value of the static pressure because the leading edge of the fuselage is robust.
- The second model has an intermediate value of the static pressure because of the engine's inlet, but it has the lowest value of the static pressure at the leading edge of the fuselage compared to the other two models.
- All three models create a relatively good distribution of the lift force on the upper surface.

From this point of view model one is better in this configuration because the shape of it disperses rapidly the drag force.

Comparison according to the vertical velocity distribution:

- All three models have a uniform distribution of the velocity around the upper and lower surface.

Comparison according to the profile of eddy viscosity distribution:

- All three models have a relatively low turbulence on the upper surface of the fuselage which can be transposed in a good design of this area.
- On the lower surface of the fuselage turbulence occur, because of the surveillance equipment.
- The third model shows the largest turbulence zone on the lower part of the trailing edge of the fuselage.

- All three models show a large zone of turbulence after the engine's inlet which can't be avoid.
- The first model shows a greater value of turbulence on the engine's inlet compared to the other two models which can be translated in a bad fluid flow in the engine.

From this point of view model two is better in this configuration because it has the fewer zones which can create turbulences.

8. Conclusion

Based on the CFD steady state analysis of the flow over the three models of UAVs the following conclusions can be drawn:

1. The second model has the lowest drag force on the leading edge but also it has the lowest internal volume, which leads to poor equipment with surveillance devices.
2. For models one and three at the front of the fuselage, a low-pressure zone is created due to the acceleration of the air fillets on the upper surface of the fuselage, which lead to the appearance of a positive momentum on the pitch axis.
3. The third model has the largest turbulence zone at the trailing edge of the fuselage compared to the other two models, which can lead to a poor flow for the propeller and make it unstable.
4. The contours of the static pressure, eddy viscosity and velocity are discussed in detail.
5. In a future attempt, the CFD analysis should be performed for different angles of attack, for a better comparison of the models.
6. The mesh has to be refined, and the convergence criterion should be raised above 1e-3 to obtain more accurate results.
7. A more accurate turbulence model, like k-ω SST, is recommended to better capture the profile of the turbulence near the wall.
8. For a better comparison of the models a transient CFD analysis should be performed, with the rotation of the propeller taken into account.

Bibliography

[1] Marin, N. and Spătaru, P. (2010), "The role and importance of UAV within the current theaters of operations", INCAS BULLETIN, Volume 2, Number 2/ 2010, pp. 66-72, DOI: 10.13111/2066-8201.2010.2.2.9;
[2] Fulghum, A. D. and Sweetman, B. (2009), "Black UAV Performs in Afghanistan", Aviation Week.com;
[3] Nehme, C. E., Cummings, M.I. and Crandall J. W. (2006), "A UAV Mission Hierarchy", Massachusetts Institute of Technology, HAL2006-09;
[4] van Blyenburgh, P. (2008) "Unmanned Aircraft Systems - The Current Situation UAS", UAS ATM Integration Workshop EUROCONTROL, Brussels, May 8;
[5] Story, A. and Gottlieb, A. (1995), "Beyond the Range of Military Operations", Military Operations, JFQ, pp. 99-104;
[6] Porock, C. (2014), "Swiss Select Hermes 900 as New UAS", AINonline, June 11;
[7] ** "Elbit Hermes 900", Wikipedia;
[8] *(2018), "Photo of russia's orion uav armed with guided munitions appears online", South Front, July 21;
[9] ** "Kronshtadt Orion", Wikipedia;
[10] Trew, J. (2012), "Northrop Grumman Unveils US Navy's MQ-4C BAMS Triton unmanned aircraft", Engadget, June 16;
[11] ** "Northrop Grumman MQ-4C Triton", Wikipedia;
[12] Kandwal, S. and Singh, S. (2012), "Computational Fluid Dynamics Study of Fluid Flow and Aerodynamic Forces on An Airfoil", Volume 01, Issue 07, ISSN: 2278-0181;
[13] Sharad, N. P. (2022), "CFD Modeling of Flow Over a Cylinder", CFD Flow Engineering;
[14] Wimshurst, A. (2020), "[CFD] The Spalart-Allmaras Turbulence Model", Fluid Mechanics 101;
[15] Kalitzin, G., Medic, G., Iaccarino, G. and Durbin, P. (2005), "Near-wall behaviour of RANS turbulence models and implications for wall functions", Journal of Computational Physics 204, 265-291;
[16] Spalart, P. R. and Allmaras, S. R.. (1992), "A One-Equation Turbulence Model for Aerodynamic Flows", 30th Aerospace Sciences Meeting and Exhibit.,AIAA Paper, 92-0439.